Article

Longitudinal Evaluation of Hyper-Reflective Foci in the Retina Following Subretinal Delivery of Adeno-Associated Virus in Non-Human Primates

Eduardo Rodríguez-Bocanegra[1,2], Fabian Wozar[1,2], Immanuel P. Seitz[1,2], Felix F. L. Reichel[1,2], Alex Ochakovski[1,2], Kirsten Bucher[1,2], Barbara Wilhelm[3], K. Ulrich Bartz-Schmidt[1], Tobias Peters[3], and M. Dominik Fischer[1–5], for the RD-CURE Consortium

[1] University Eye Hospital, Centre for Ophthalmology, University Hospital Tübingen, Tübingen, Germany
[2] Institute for Ophthalmic Research, Centre for Ophthalmology, University Hospital Tübingen, Tübingen, Germany
[3] STZ Eye Trial at the Centre for Ophthalmology, University Hospital Tübingen, Tübingen, Germany
[4] Oxford Eye Hospital, Oxford University NHS Foundation Trust, Oxford, UK
[5] Nuffield Laboratory of Ophthalmology, Department of Clinical Neurosciences, University of Oxford, Oxford, UK

Purpose: The purpose of this study was to evaluate whether clinical grade recombinant adeno-associated virus serotype 8 (rAAV8) leads to increased appearance of hyper-reflective foci (HRF) in the retina of non-human primates (NHPs) following subretinal gene therapy injection.

Methods: Different doses of rAAV8 vector (rAAV8. human phosphodiesterase 6A subunit (hPDE6A) at low dose: 1×10^{11} vector genomes (vg), medium dose: 5×10^{11} vg, or high dose: 1×10^{12} vg) were injected subretinally into the left eyes of NHPs in a formal toxicology study in preparation of a clinical trial. Right eyes received sham-injection. After 3 months of in vivo, follow-up retinal sections were obtained and analyzed. The number of HRF on spectral domain-optical coherence tomography (SD-OCT) volume scans were counted from both eyes at 30 and 90 days.

Results: Animals from the high-dose group showed more HRF than in the low ($P = 0.03$) and medium ($P = 0.01$) dose groups at 90 days. There was a significant increase in the mean number of HRF in rAAV8-treated eyes compared with sham-treated eyes at 90 days ($P = 0.02$). Sham-treated eyes demonstrated a nonsignificant reduction of HRF numbers over time. In contrast, a significant increase over time was observed in the rAAV8-treated eyes of the high dose group ($P = 0.001$). The presence of infiltrating B- and T-cells and microglia activation were detected in rAAV8-treated eyes.

Conclusions: Some HRF in the retina appear to be related to the surgical trauma of subretinal injection. Although HRF in sham-treated retina tends to become less frequent over time, they accumulate in the high-dose rAAV8-treated eyes. This may suggest a sustained immunogenicity when subretinal injections of higher doses of rAAV8 vectors are applied, but it has lower impact when using more clinically relevant doses (low and medium groups).

Translational Relevance: An increase or persistence of HRFs following retinal gene therapy may indicate the need for immunomodulatory treatment.

Introduction

Recombinant adeno-associated viral (rAAV) vectors have been used for retinal gene therapy for more than 10 years with positive efficacy and safety results. However, despite this success, the number of independent study reports suggesting local and systemic immune responses after ocular rAAV delivery is increasing.[1–6]

Depending on factors, such as dose, route of administration, rAAV capsid, and transgene expression, discrete hyper-reflective elements or hyper-reflective foci (HRF), might appear in spectral-domain optical coherence tomography (SD-OCT) scans as a potential indicator of a cellular immune response in the retina.[5] Even though the appearance of HRF after gene therapy remains ill defined, the presence of HRF in the outer retinal layers[7] could be a potential indicator of immune responses in the form of cellular activation/infiltration by immune-competent cells[6,8,9] associated to the surgical procedure, the rAAV treatment, or a combination of both. Coscas et al. suggested that HRF could represent microglia cell activation when they first described the existence of HRF in age-related macular degeneration (AMD).[10] Vujosevic et al. suggested that HRF could be aggregates of activated microglial cells in patients with diabetic macular edema and its appearance was also related to an increased inflammation in the retina.[11,12]

Previous studies showed that gene therapy using rAAV may induce retinal toxicity in preclinical studies in the form of loss of photoreceptors causing the thinning of the outer nuclear layer (ONL)[13] or migration of retinal pigment epithelial (RPE) cells into the neuroretina.[8,14] It is also clear that the surgical intervention causes cell damage at the retinotomy, where a blunt needle of ca. 130 μm outer diameter penetrates the neuroretinal tissue (ca. 260 μm thickness), which leads to changes on the tissue, cellular, and molecular levels.[5]

To reduce the number of animals used in studies and in line with the principle of the 3Rs (reduce, reuse, and recycle),[15] we utilized data (tissue and images) collected for formal toxicology assessment of a gene therapy drug developed for the treatment of patients with phosphodiesterase 6A subunit (PDE6A) related retinitis pigmentosa. This treatment is currently being tested in a clinical trial and consists of a clinical grade rAAV8.hPDE6A vector. Using these data, we studied whether injection of rAAV8 would induce more HRF compared to sham treatment at different doses and time points. We also aimed to explore how HRF relates to changes in the ONL thickness and to confirm the identity of the HRF by histology and immunofluorescence analysis.

Materials and Methods

Animals

This study used data obtained in a formal toxicology assessment for an investigational new drug (rAAV8.hPDE6A vector) developed to treat patients with PDE6A related retinitis pigmentosa. The use of these data allowed us to reduce the number of animals needed to study this important question in line with the principles of the 3Rs.

The study was in compliance with the German Animal Welfare Act, in accordance with the ARVO Statement for the Use of Animals in Ophthalmic and Vision Research, and approved by the local Institutional Animal Care and Use Committee. It was conducted at primate facilities of Covance according to good laboratory practice (GLP) and additional data analysis was performed at the Centre for Ophthalmology Tübingen. Twelve cynomolgus monkeys (*Macaca fascicularis*) were included in the study using an equal number of males and females. However, non-GLP work beyond the toxicology study was done in the analysis shown here.

Pre-Operative Preparation

Before surgery, animals were anesthetized and sedated with ketamine and medetomidine for intubation and isoflurane narcosis for procedure. In addition, periorbital regions were cleaned with povidone iodine and sterile surgical drapes; and a pediatric lid speculum was applied to the operated eye.

Subretinal Injection

Surgery (all performed by author M.D.F.) was highly standardized and bleb location documented in each animal. A temporal canthotomy was applied when necessary. Three sclerotomies were made 1 to 2 mm posterior to the limbus after transillumination confirmed location of pars plana. A pars plana vitrectomy was performed. Induction of a localized retinal detachment was performed with a subretinal injection of balance salt solution (BSS; Alcon) using a 41-gauge cannula (DORC 1270.EXT). The right eyes received a single injection of 170 μl of clinical grade rAAV8.hPDE6A vector, whereas the left eyes received 170 μl of BSS. Injection speed was regulated by the surgeon via a foot-pedal-controlled semi-automatic

system attached to the vitrectomy machine resulting in a controlled bleb formation with the injection of 170 µl completed in circa 1 minute. The actual injection pressure was not recorded for each animal, however, the setting also used in a study on an optimized injection system (range of 0–150 kPa)[16] was maintained across all animals. No fluid-air exchange was performed, but the infusion was active while the vitrectomy probe was used to wash out the vitreous cavity for 3 minutes after completion of the bleb.

Dosing

In our rAAV8 vectors, hPDE6A was expressed under the human rhodopsin kinase promoter (RK). Three different groups were created regarding the level of the injected dose. Four animals were included per group (50% males and 50% females). In total, the low-dose group received 1×10^{11} vg (group 1) of clinical grade rAAV8.hPDE6A vector, the medium-dose group received 5×10^{11} vg (group 2), and the high-dose group received 1×10^{12} vg (group 3).

Immunosuppressive Treatment

Just after surgery, subconjunctival piperacillin and dexamethasone (2 mg) were administered to the operated eyes. During the first week after surgery, there was a postoperative local treatment consisting of eyedrops vigamoz (0.5% moxifloxacin) three times daily in both eyes and prednifluid (10 mg/mL prednisolonacetat) three times daily in both eyes. Systemic immunosuppression was carried out with prednisolonacetat at 1 mg/kg (intramuscular) from 2 days prior to surgery until day 5 after surgery.

Postoperative Follow-Up

All animals were periodically assessed with a complete ophthalmic examination. Before subretinal injections, all animals were evaluated in order to assess the state of the retina and rule out ocular morbidities. Animals were evaluated at days 30, 60, and 90 after subretinal injections. Ophthalmological examinations of the animals were done while they were under sedation. Assessment of the retinas was performed with infrared (IR), fundus autofluorescence (FAF; excitation filter at 488 nm) and SD-OCT imaging using the Spectralis HRA + OCT (Heidelberg Engineering, Heidelberg, Germany). SD-OCT examinations were performed with tracking activated from baseline if possible. Euthanasia was carried out under sedation with an intramuscular injection of ketamine hydrochloride, followed by an intravenous injection of sodium pentobarbitone overdose.

Counting and Distribution of Hyper-Reflective Foci

HRF were defined as discrete and well-circumscribed elements of equal or higher reflectivity than the RPE layer on SD-OCT. As the bleb was always formed in the superior hemiretina following a retinotomy along the superior-temporal arcade, it was possible to reliably identify B-scans from within the bleb area (superior) and corresponding (same orientation and eccentricity) B-scans from the nondetached retina. Therefore, HRF were counted in areas in and outside of the bleb for both right and left eyes from all animals at days 30 and 90 after treatment using 9-mm SD-OCT volume scan images (no HRF were found at baseline). The HRF were counted manually (Fig. 1) by three independent and masked examiners (authors E.R.B., F.W., and I.S.) using a cell counter plugin of FIJI software (ImageJ software, provided for free by the National Institutes of Health, Bethesda, MD, USA, and available at https://fiji.sc/). The HRF were subdivided according to the retinal layers: ONL and outer retina (from external limiting membrane to RPE [included]). In order to create distribution maps, the images from animals that were close to the mean HRF were selected as representative examples. All HRF from those animals were plotted on IR and FAF images by marking the position of each individual HRF from SD-OCT images.

Outer Nuclear Layer Thickness

Thickness of ONL was measured at baseline and at days 30 and 90 after treatment using 6-mm SD-OCT volume scan images. The measurements were made at 2 mm superior to the fovea (in the bleb area) with Spectralis thickness maps tool and using the 1-, 2- and 3-mm early treatment diabetic retinopathy study (ETDRS) grid (area = 7.065 mm^2).

Histology and Immunohistochemistry

NHP eyes were fixed in 4% paraformaldehyde for 24 hours at 4°C. The eye-cups were dehydrated in different concentrations of ethanol and xylol. Then, the eye-cups were embedded in paraffin for posterior sectioning. Slides for anatomic evaluation were processed using hematoxylin and eosin (H&E) staining and assessed under a light microscope.
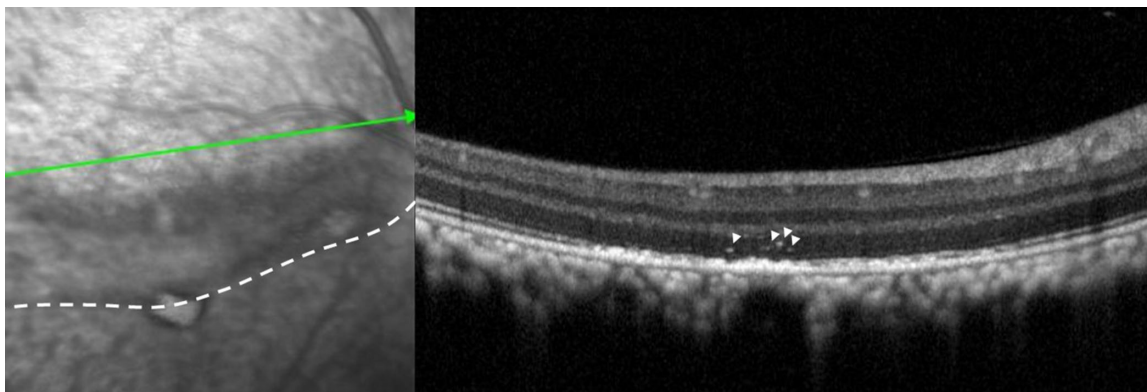
Figure 1. SD-OCT image of HRF in a sham-treated eye of NHP. The 30 degrees fundus IR image with overlying position of B-Scan (*left panel, green line*) and cross-sectional SD-OCT B-scan (*right panel*) demonstrate the appearance of HRF in the ONL (*arrow heads*) within the bleb area (*white dashed line*) 30 days after subretinal injection. HRF, hyper-reflective foci; IR, infrared; NHP, non-human primate; ONL, outer nuclear layer; SD-OCT, spectral-domain optical coherence tomography.

Table 1. List of Antibodies Used in This Study

Antibody	Marker	Species	Dilution	Further Information
Primary	Anti-human CD20	Mouse	1:200	Dako, M0755
Primary	Anti-human CD3	Rabbit	1:100	Abcam, ab5690
Primary	Anti-human Iba-1	Rabbit	1:500	Wako, 019-19741
Primary	Anti-human CD68	Mouse	1:50	Dako, M0814
Primary	Anti-human RPE65	Rabbit	1:6000	Abcam, ab231782
Secondary	Anti-mouse IgG 488	Donkey	1:500	Abcam, ab150105
Secondary	Anti-rabbit IgG 568	Donkey	1:1000	Abcam, ab175470

For immunohistochemistry, sections were deparaffinized using different concentrations of xylol and ethanol. Sections were heated in a pressure cooker with an antigen unmasking solution (VECTOR Laboratories) for 2 minutes and then washed twice with phosphate buffered saline (PBS) for 5 minutes each. For immunofluorescence, sections were blocked with 10% donkey serum + 0.05% Tween 20 in PBS for 1 hour at room temperature, continued by the same washing step. The primary antibody (Table 1) was incubated 1 hour at room temperature, and then washed twice with 0.05% Tween 20 in PBS for 5 minutes each. Secondary antibody (see Table 1) was incubated for 2 hours at room temperature. After another two wash steps with 0.05% Tween 20 in PBS for 5 minutes each, sections were mounted with 1-2 drops of antifade mounting medium with DAPI (VECTOR Laboratories) and coverslip. For immunohistochemical permanent staining, sections were blocked in BIOXALL blocking solution (VECTOR Laboratories) for 10 minutes and washed 3 times with tris-HCl buffered saline (TBS) for 5 minutes each. Then, the sections were incubated with 2.5% horse serum for 20 minutes and

retinoid isomerohydrolase (RPE65) primary antibody for another 30 minutes. After washing 3 times with TBS 5 minutes each, sections were incubated 30 minutes with ImmPRESS – AP Reagent (horse anti-rabbit IgG; VECTOR Laboratories) and washed 3 more times in TBS. After this, there was an incubation with ImmPACT Vector Red (VECTOR Laboratories) for 30 minutes in the dark followed by 3 washing steps with tap water and an incubation with hematoxylin (VECTOR Laboratories) for 25 seconds. Finally, after washing three more times with tap water, the sections were dehydrated in different concentrations of ethanol and xylol and mounted with mounting media and coverslip.

When sections were dried, pictures were taken using an Axio Imager Z1 microscope (Zeiss, Germany), and processed using ZEN 3.2 (Blue edition).

Data Analysis

Statistical analysis was carried out using GraphPad Prism (version 8.0.0, GraphPad Software, San Diego, CA, USA, www.graphpad.com) and Excel (Microsoft
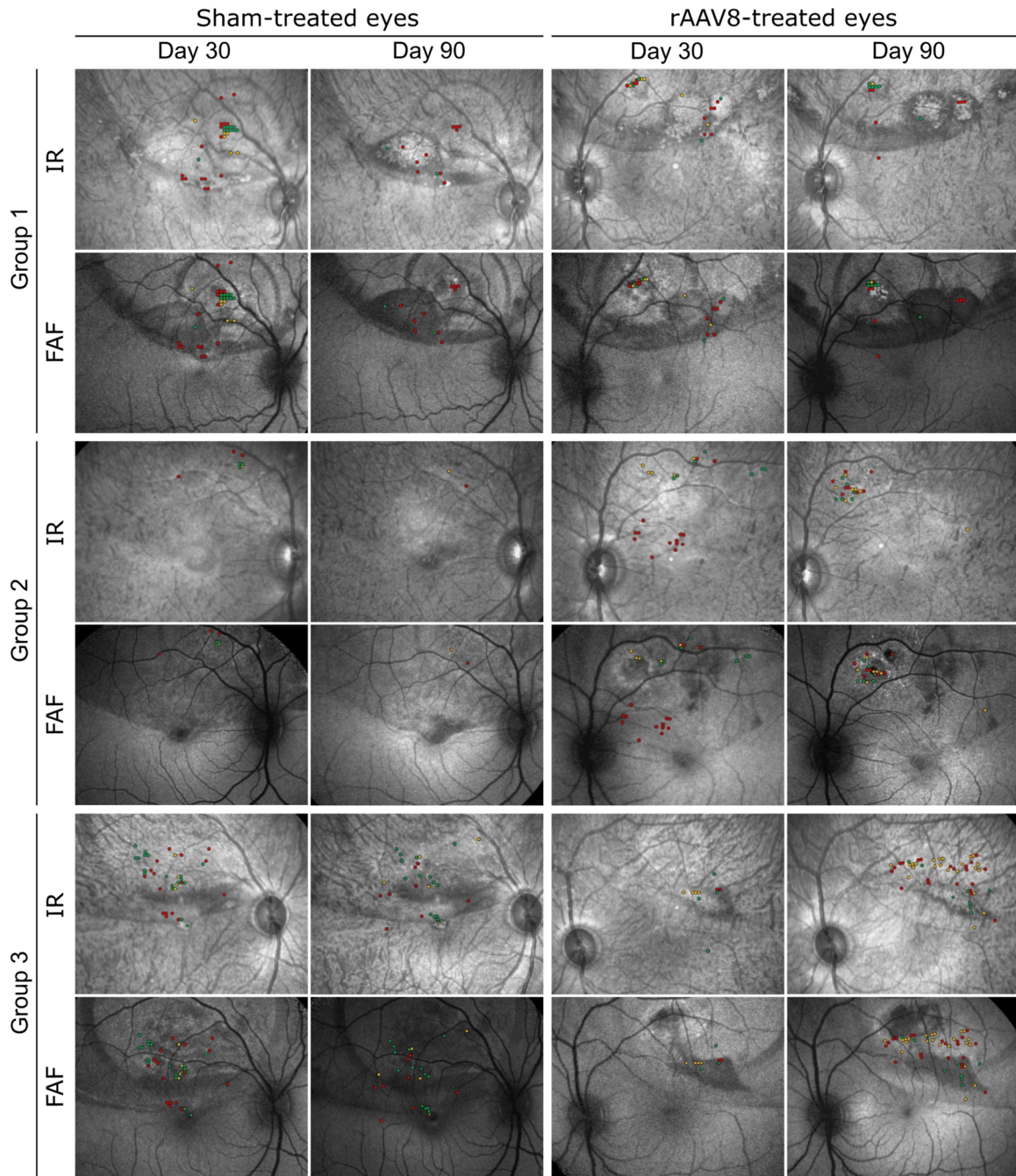
Figure 2. Representative distribution maps of HRF in the retina of NHPs 30 and 90 days after subretinal injection of BSS (sham) or different doses of rAAV8. HRF are plotted on IR and FAF images in different colors. *Green dots* = HRF were identified by three observers; *yellow dots* = HRF were identified by two observers; *red dots* = HRF were identified by one observer. FAF, fundus autofluorescence; Group 1, low-dose group; Group 2, medium-dose group; Group 3, high-dose group; HRF, hyper-reflective foci; IR, infrared; NHP, non-human primate.

Office 2016). Differences in the number of HRF and ONL thickness between each visit were evaluated using 2-way ANOVA followed by Tukey's honestly significant difference (HSD) post hoc test. Differences between dose groups and between sham- and rAAV8-treated eyes from the same dose group were evaluated using 2-way ANOVA followed by Sidak's correction post hoc analysis. Interexaminer interclass correlation coefficient (ICC) was performed to determine the reproducibility of the HRF counting. The presented results are shown as mean ± standard deviation. *P* values less than 0.05 were considered as statistically significant.

Figures were created using both FIJI and Inkscape (version 1.0, https://inkscape.org/).

Table 2. Mean Number of HRF in Sham- Versus rAAV8-Treated Eyes Per Dose Group After 30 and 90 Days Post-Treatment Using 2-Way ANOVA and Sidak's Correction Post Hoc Analysis

			30 Days After Treatment			90 Days After Treatment		
Dose Group	Dose (vg)	n	Right Eye (Sham)	Left Eye (rAAV8)	P Value	Right Eye (Sham)	Left Eye (rAAV8)	P Values: ≤0.05[*]
1 (low)	1E + 11	4	20.7 ± 23.4	11.4 ± 17.2	0.60	10.4 ± 8.7	16.4 ± 20.5	0.91
2 (medium)	5E + 11	4	28.2 ± 27.4	18.8 ± 14.8	0.59	7.2 ± 9.2	13.4 ± 12.5	0.90
3 (high)	1E + 12	4	21.3 ± 24.8	5.9 ± 4.6	0.19	14.4 ± 16.0	43.2 ± 51.8	0.02[*]

[*]*P* values = ≤0.05.

Table 3. Multiple Comparisons of Mean Difference in the Number of HRF in Sham- and rAAV8-Treated Eyes Among the Dose-Groups Using Tukey's HSD Post Hoc Analysis

					95% CI of the Diff.		
Eye	Time Point	Groups (J)	Groups (K)	Mean Diff. (J-K)	Lower	Upper	P Value
Sham	30 days	Group 1	Group 2	−7.50	−26.79	11.79	0.62
			Group 3	−0.67	−19.96	18.63	0.99
		Group 2	Group 3	6.83	−12.46	26.13	0.67
	90 days	Group 1	Group 2	3.25	−16.04	22.54	0.91
			Group 3	−4.00	−23.29	15.29	0.87
		Group 2	Group 3	−7.25	−26.54	12.04	0.64
rAAV8	30 days	Group 1	Group 2	−7.33	−31.97	17.30	0.76
			Group 3	5.50	−19.14	30.14	0.85
		Group 2	Group 3	12.83	−11.80	37.47	0.43
	90 days	Group 1	Group 2	3.00	−21.64	27.64	0.95
			Group 3	−26.75	−51.39	−2.11	0.03[*]
		Group 2	Group 3	−29.75	−54.39	−5.11	0.01[*]

CI, confidence interval.
[*]*P* values = ≤0.05.

Results

A total of 24 eyes from 12 healthy NHPs were included in the study. After analyzing SD-OCT volume scans, HRF were present in 12 of 12 (100%) sham-treated eyes and also in 12 of 12 (100%) rAAV8-treated eyes after 30 and 90 days. There was a high degree of ICC (81%) on the number of HRF in the ONL in this study. However, HRF counting in the outer retina had a high degree of discrepancy among assessors (<40%), so this analysis was not further pursued.

HRF were mostly detected surrounding the retinotomy site and also in transition areas between the bleb border and nondetached retina as shown in the HRF distribution maps (Fig. 2). The mean number of all HRF (including HRF observed by only one assessor; see Fig. 2) in sham- versus rAAV8-treated eyes after 30- and 90-days post-treatment is summarized in Table 2. These data show that there are no significant differences in the number of HRF between sham- and rAAV8-treated eyes neither at 30 days nor at 90 days post-treatment in groups 1 and 2. However, in group 3, there is a significant difference in the number of HRF at 90 days between sham- and rAAV8-treated eyes with an increased number of HRF in the rAAV8-treated eyes.

The number of HRF was also compared between the dose groups (Table 3). There were significant differences in the number of HRF at 90 days between eyes treated with low and high dose (16.4 ± 20.5 vs. 43.2 ± 51.8, $P = 0.03$) and between medium and high dose rAAV8 (13.4 ± 12.5 vs. 43.2 ± 51.8, $P = 0.01$).

In order to study its kinetics, the number of HRF was compared between time points (i.e. 30 vs. 90 days; Table 4). There were two situations where significant differences were found between time points. The first one was observed in the sham-treated eyes of group 2 where the number of HRF was significantly higher at day 30 than at day 90 (28.2 ± 27.4 vs. 7.2 ± 9.2,

Table 4. Multiple Comparisons of Mean Difference in the Number of HRF in Sham- and rAAV8-Treated Eyes Among the Two Different Time Points Using Sidak's Correction Post Hoc Analysis

Eye	Groups	Time Point (J)	Time Point (K)	Mean Diff. (J-K)	95% CI of the Diff. Lower	95% CI of the Diff. Upper	P Value
Sham	Group 1	30 days	90 days	10.25	−4.59	25.09	0.25
	Group 2			21.00	6.16	35.84	0.003[**]
	Group 3			6.92	−7.92	21.75	0.58
rAAV8	Group 1	30 days	90 days	−5.00	−28.52	18.52	0.93
	Group 2			−5.33	−18.18	28.85	0.92
	Group 3			−37.25	−60.77	−13.73	0.001[**]

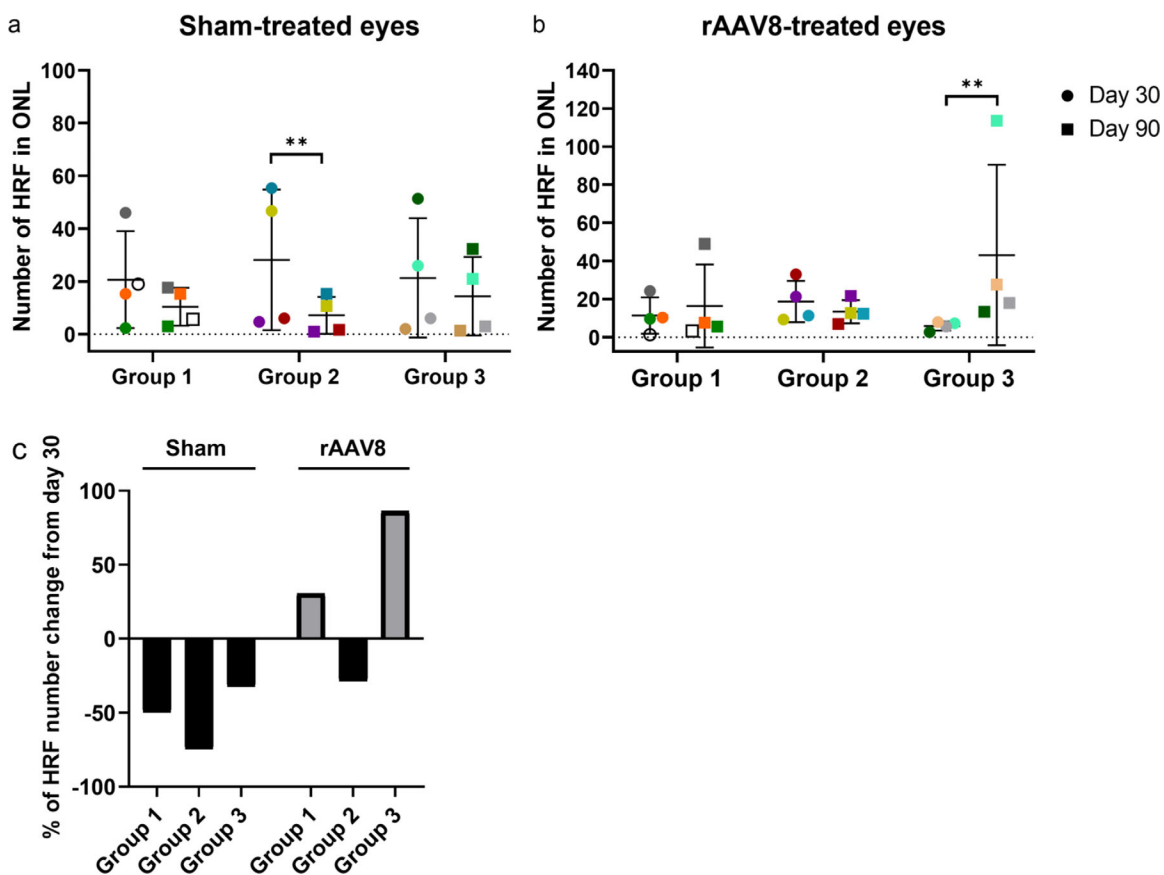CI, confidence interval.
[**]P values = ≤0.01.

Figure 3. Kinetics of HRF of over time in sham- (**a**) and rAAV8-treated (**b**) eyes. Data are shown as mean ± standard deviation for the 3 groups at days 30 and 90 post-subretinal injection. Each colored symbol represents one animal (4 per group, P value = ≤0.01: **). Graphic representation of the percentage of mean change in the number of HRF normalized to 30-days measurements (**c**). Values below 0 indicate a decrease in the percentage of the number of HRF from day 30 to day 90; and values above 0 indicate an increase of HRF. Group 1, low-dose group; Group 2, medium-dose group; Group 3, high-dose group; HRF, hyper-reflective foci; ONL, outer nuclear layer.

P = 0.003; Fig. 3a). In addition, a general trend in the reduction of the number of HRF was observed in a nonsignificant way in the sham-treated eyes of the three dose groups. In contrast, the rAAV8-treated eyes of group 3 demonstrated an increase of HRF over time with significantly higher numbers at day 90 versus at day 30 (43.2 ± 51.8 vs. 5.9 ± 4.6, P = 0.001' Fig. 3b). Moreover, the data also show that there is a nonsignificant difference in the number of HRF in rAAV8-treated eyes in groups 1 and 2 over time (see

Table 5. Multiple Comparisons of Mean Difference in the Thickness of ONL (μm) in Sham- and rAAV8-Treated Eyes Among the Three Different Time Points Using Tukey's HSD Post Hoc Analysis

| Eye | Groups | Time Point (J) | Time Point (K) | Mean Diff. (J-K) | 95% CI of the Diff. | | P Value |
					Lower	Upper	
Sham	Group 1	BSL	30 days	3.27	0.56	5.89	0.015[*]
		30 days	90 days	−1.68	−4.14	0.78	0.23
	Group 2	BSL	30 days	1.47	0.29	2.65	0.013[*]
		30 days	90 days	2.60	1.60	3.60	<0.0001[***]
	Group 3	BSL	30 days	12.17	5.31	19.03	0.0003[***]
		30 days	90 days	−1.31	−5.11	2.48	0.68
rAAV8	Group 1	BSL	30 days	−0.23	−2.26	1.81	0.96
		30 days	90 days	−1.32	−3.40	0.74	0.27
	Group 2	BSL	30 days	−1.28	−2.64	0.09	0.07
		30 days	90 days	3.85	2.54	5.17	<0.0001[***]
	Group 3	BSL	30 days	−2.294	−5.95	1.37	0.29
		30 days	90 days	2.18	−1.67	6.04	0.36

CI, confidence interval.
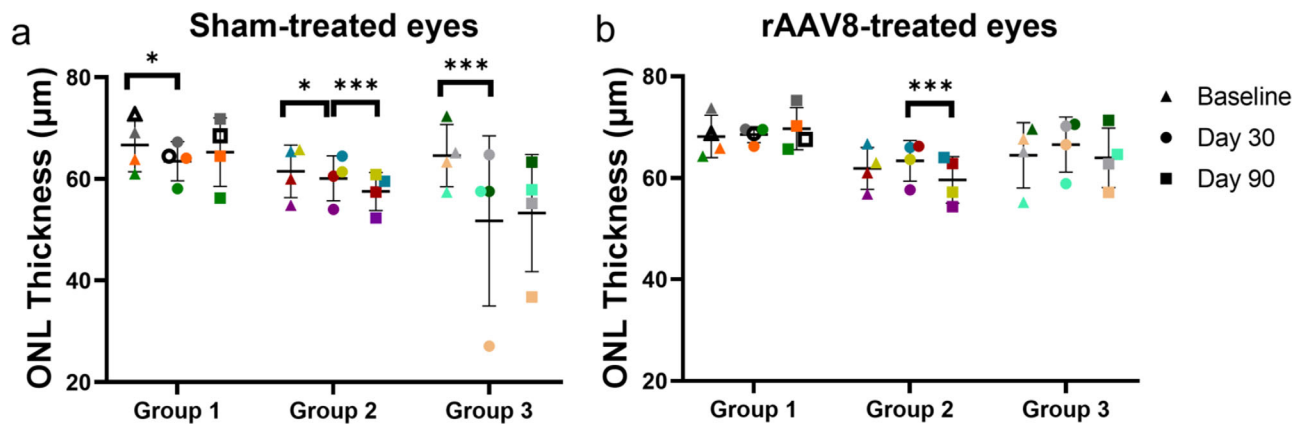[*]*P* values = ≤0.05.
[***]*P* values = ≤0.001.

Figure 4. Thickness of ONL over time in sham- (**a**) and rAAV8-treated (**b**) eyes. Data are shown as mean ± standard deviation for the 3 groups at days 30 and 90 post-subretinal injection. Each colored symbol represents one animal (4 per group, *P* values = ≤0.05: *; ≤0.001: ***). Group 1, low-dose group; Group 2, medium-dose group; Group 3, high-dose group; ONL, outer nuclear layer.

Table 4). Raw data of HRF number from each animal was summarized in Supplementary Table S1.

Figure 3c shows the changes in the numbers of HRF, normalized for 30-day measurements, in the sham- and rAAV8-treated eyes per group. In sham-treated eyes from groups 1, 2, and 3, there was a reduction in the number of HRF corresponding to a mean loss of 49%, 74%, and 32%, respectively. In parallel, in rAAV8-treated eyes, a reduction in the number of HRF was also found in group 2 corresponding to a mean loss of 28%, but groups 1 and 3 showed an increase in the HRF number corresponding to a mean gain of 30% and 86%, respectively.

The thickness of the ONL in the sham-treated eyes of groups 1, 2, and 3 was significantly reduced 30 days after subretinal injection (*P* = 0.015, 0.013, and 0.0003, respectively; Table 5, Fig. 4a). After 90 days, groups 1 and 3 showed no differences in ONL thickness compared to day 30 (*P* = 0.23 and 0.68, respectively), but group 2 was again significantly reduced (*P* = <0.0001). In contrast, the thickness of the ONL in the rAAV8-treated eyes did not change in any group after the first 30 days post subretinal injection (*P* = 0.96, 0.07, and 0.29, for groups 1, 2, and 3; see Table 5, Fig. 4b). At day 90, the thickness of the ONL was significantly reduced in group 2 (*P* = <0.0001) but no

such change was observed in the other two groups (P = 0.27 and 0.36, for groups 1 and 3). Raw data of ONL thickness from each animal was summarized in Supplementary Table S2.

To explore a likely histological equivalent of the HRF, immunohistochemistry analysis was performed on the NHP retinas. An accurate correlation between horizontal SD-OCT scans and vertical retinal sections was not possible due to their respective spatial orientations and likely artifacts in the processing of the eye cups. However, the sections were labeled with the macrophage marker CD68, the B-cell marker CD20 and the T-cell marker CD3, and microglia activation was labeled with Iba-1 and RPE cells with RPE65 with the aim to perform a semiquantitative comparison.

In sham-treated eyes, staining with the immune cell markers CD20, CD3, and CD68 was negative in all the groups even in areas nearby the retinotomy (Figs. 5a–l). H&E staining did not show any irregularities of the tissue, meaning that these eyes did not exhibit any distinctive evidence of inflammatory cell infiltrate in the retina (despite the frequency of HRF evident from the SD-OCT data). However, both sham- and rAAV8-treated eyes showed positive Iba-1 staining in areas close to the retinotomy site (bleb area), whereas Iba-1 staining was negative in nontreated areas of the same retinas suggesting increased microglia activation in the bleb area (data not shown). Iba-1 staining in areas near the retinotomy site was much more evident in rAAV8-treated eyes than in sham-treated eyes (Figs. 5m–x). B- and T-cells were found in the retina of 4 out of 12 animals: 1 from group 1 and 3 animals from group 3, but not detected in animals from group 2. The macrophage marker CD68 was only present in one of the animals from group 3. No migration of RPE cells was detected using the RPE65 specific antibody.

The presence of cell infiltrates in the retina was observed first in H&E staining of 2 rAAV8-injected eyes from groups 1 and 3. In both animals, perivascular infiltrates appeared surrounding blood vessels (Figs. 6a–j) and, in the animal from group 1, there was also a subretinal cell infiltration (Figs. 6k–t) in the area where the retinotomy was performed. Infiltrates were located in areas near the retinotomy site. The majority of the cells of the infiltrate were positive for immune cell markers. B- and T-infiltrating cells together with activated microglia cells were the predominant immune cells in both perivascular and subretinal infiltrates. The integrity of the RPE layer was normal in all animals from all groups except for the area where the subretinal infiltrate was present.

Discussion

In this study, we explore whether the addition of rAAV8 to the surgical trauma of subretinal injection influences frequency or temporal dynamics of HRF as a potential indicator of immune cell activation / infiltration following subretinal injection. We utilized data from a formal toxicology study in NHPs as a highly relevant model while striving to maximize use of the data set according to the principles of the 3Rs. Results demonstrate that (i) the surgical procedure of subretinal injection by itself induced the appearance of HRF in the ONL; (ii) while the number of HRF decreased (in a nonsignificant way) in the sham group, the number of HRF increased over time in the rAAV8 treated eyes and became significantly higher 90 days after subretinal injection in eyes receiving a high dose of rAAV8; (iii) while differences in ONL thickness were related to the surgical procedure rather than the addition of viral vectors; (iv) immune cell infiltration was detected only in retinal sections from rAAV8-treated eyes, but not in sham-treated eyes; and (v) while microglia cell activation was evident in all eyes.

There are many ocular disorders that can present with retinal HRF, such as AMD, uveitis, diabetic macular edema, retinitis pigmentosa, or Stargardt's disease among others.[17–21] However, very little is known about the appearance of HRF in eyes after subretinal gene therapy with rAAV. To our knowledge, HRF have only been described in three different clinical studies using rAAV. The first one from Reichel et al.,[8] a retinal gene therapy trial for CNGA3-based achromatopsia, describes a patient who had received a single subretinal injection of rAAV8 (1×10^{10} vg) and developed discrete HRF 2 weeks after the surgery. In the second one from Dimopoulos et al.,[7] a clinical trial to assess the safety of rAAV2, SD-OCT images revealed that a patient treated with 1×10^{11} vg developed HRF in the outer retinal layers 1 month after the treatment. In the third study from Cehajic-Kapetanovic et al.,[6] a first-in-human gene therapy trial on X-linked retinitis pigmentosa using rAAV8, seven patients from the high-dose group (dose between 6×10^{10} vg and 4×10^{11} vg) showed the presence of HRF in the treated eyes after subretinal injections. The authors also reported that these hyper-reflective subretinal lesions were related to gene therapy and were leading to transient regression of retinal function.[6] However, in the three studies, HRF resolved after oral steroid treatment meaning that HRF had a dynamic component.

In the present study, the animals followed an immunosuppressive treatment during 7 days in total. It differs from immunosuppression regimens in humans,
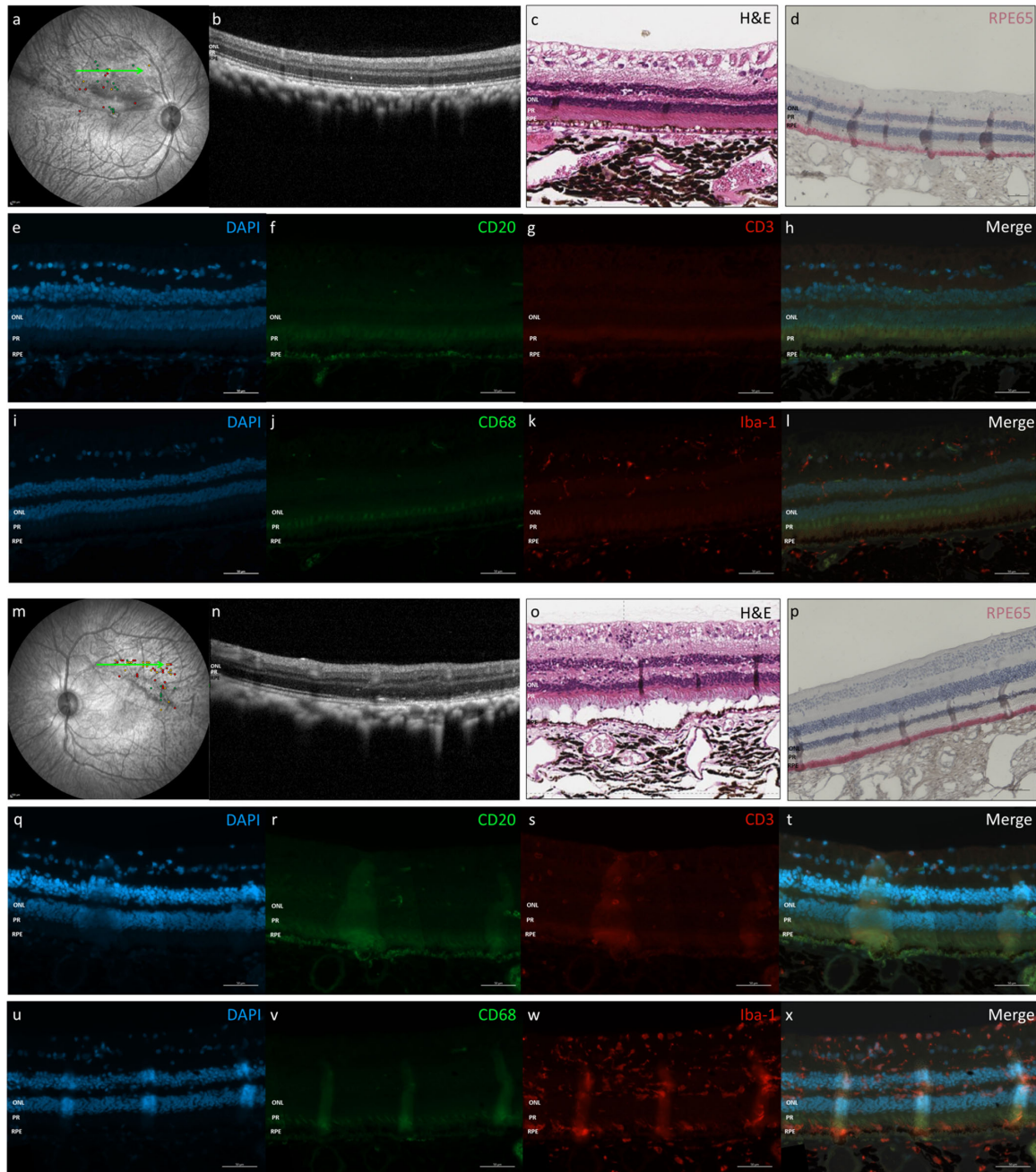
Figure 5. Immunohistochemical analysis of sham- (**a–l**) and rAAV8-treated (**m–x**) eyes from group 3. The 60 degrees fundus IR image showing the representative HRF distribution maps (**a, m**) with overlying position of B-scan (*green line*) and cross-sectional SD-OCT B-scans (**b, n**) demonstrate the appearance of HRF within the treated area 90 days after subretinal injection. Normal H&E staining of an area close to the SD-OCT scan (**c, o**). Immunohistochemical permanent staining of RPE65 shows the integrity of the RPE layer (**d, p**). B- and T-cells (CD20$^+$ and CD3$^+$ cells, respectively) were not detected in the sham treated eyes (**e–h**) but they were found in the rAAV8 treated eyes (**q–t**). The macrophage marker CD68 was not detected neither in the sham- (**j**) nor in rAAV8-treated (**v**) eyes. However, microglia cells were more active in rAAV8-treated eyes (**w**) than in sham-treated eyes (**k**). Scale bar: 50 μm. HRF, hyper-reflective foci; H&E, hematoxylin and eosin; IR, infrared; ONL, outer nuclear layer; PR, photoreceptors; RPE, retinal pigment epithelium; SD-OCT, spectral-domain optical coherence tomography.

where patients may receive immunosuppressive treatment for longer (2 to 4 weeks), including a tapering period of dose,[6–8] or in a Pro Re Nata (PRN) regimen (RGX-314 trial, NCT03066258). We tried to find a balance that would optimize animal welfare (steroids had to be given by intramuscular injections in NHPs). These differences may suggest a higher probability in order to have immune responses in the retinas of the
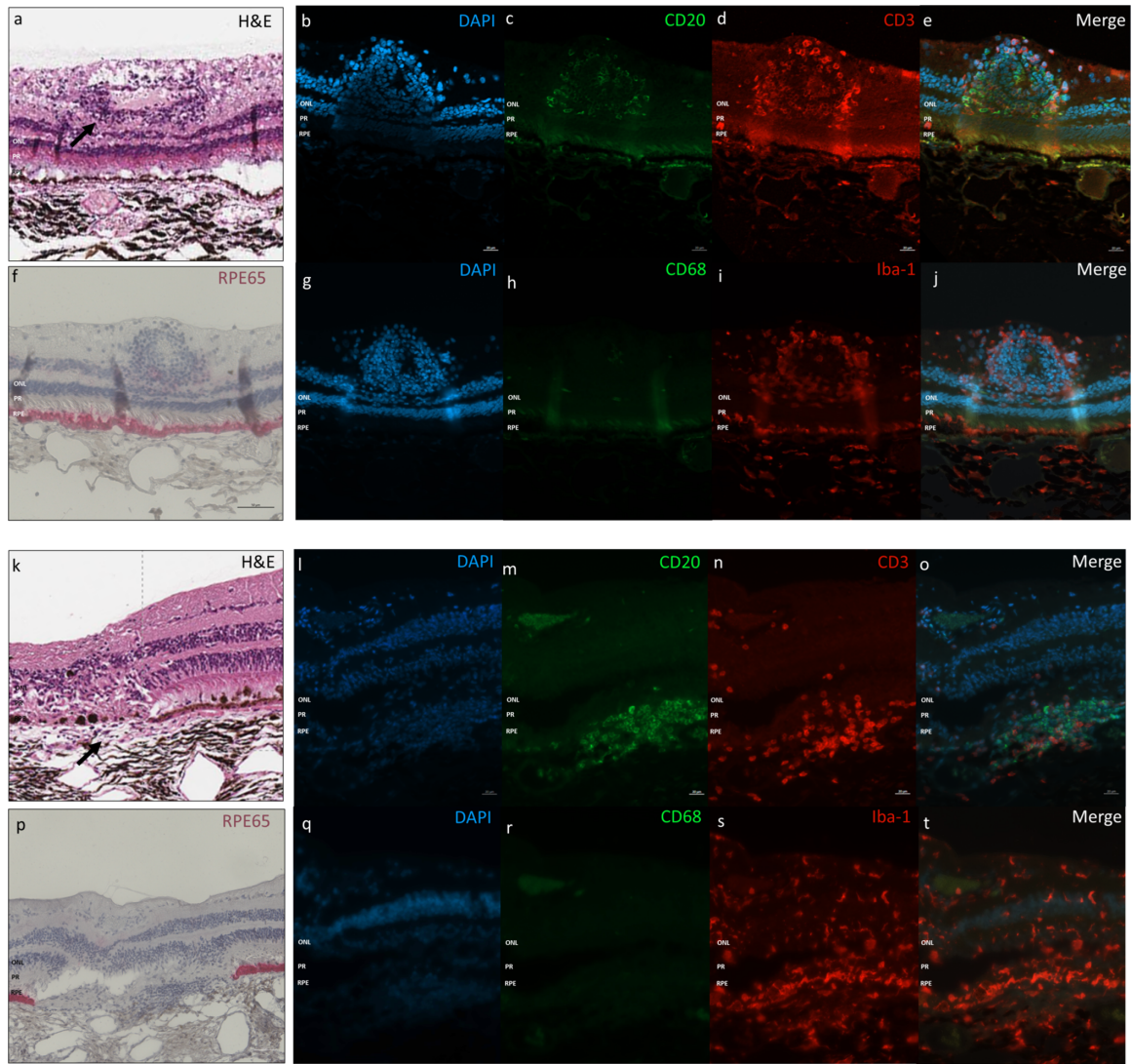
Figure 6. Immune retinal infiltrates found in perivascular (**a–j**) and subretinal (**k–t**) areas of animals from group 3 and group 1, respectively. H&E staining shows the appearance of leukocytic cells infiltration in the perivascular area of a retinal blood vessel **a** (**black arrow**) and between the neural retina and the choroid **k** (*black arrow*). RPE65 staining shows the state of the RPE layer **f** and **p** being completely absent in the area where the subretinal infiltrate is present **p**. CD20+ and CD3+ cells **b** to **e** and **l** to **o** together with microglia activation **i** and **s** were found in both types of infiltrates. The macrophage marker CD68 was only detected in the perivascular infiltrate **h**. Scale bar: 30 μm. H&E, hematoxylin and eosin; ONL, outer nuclear layer; PR, photoreceptors; RPE, retinal pigment epithelium.

animals at earlier time points (30 days). Interestingly, HRF appeared in all the eyes of the animals 30 days after injection using a 7-day immunosuppressive treatment, whereas in Reichel et al.[8] and Dimopoulos et al.,[7] HRF only appeared in 1 patient after 30 days of injection using immunosuppressive treatment for a longer period of time. Thus, the duration of the immunosuppressive treatment could be a factor to consider in order to avoid the appearance of HRF at earlier time points after treatment. It is worth mentioning that the available evidence suggests that the presence or titer of neutralizing antibodies do not affect the outcome of a subretinal application of AAV based gene therapies.[5,22]

The clinical observations of the three mentioned clinical studies are congruent with our results in the present study. There was a trend indicating a general reduction in the number of HRF in the sham-treated eyes in all groups with a significant reduction in group 2. As there were not viral particles in the sham-treated eyes, the appearance of HRF was most likely due to the surgical trauma associated with the subretinal injection. In contrast, rAAV8-treated eyes from 2 out of 3 dose groups showed an increase in the HRF number over time. Specifically, there was a significant increase between 30 and 90 days after surgery in the high-dose group (1×10^{12} vg). This kinetic has been also

observed in experiments using rats, in which, upon intravitreal injections of rAAV2, there was an increase in the number of HRF in the retina.[9]

The observed deviations in our results may well reflect variability in the surgery. A difference in surgical trauma could contribute to a difference in numbers of HRF that potentially becomes enhanced in presence of high doses of rAAV8 at later time points. Although four animals per group was deemed sufficient for the main purpose of the study (assess toxicity), increasing the number would certainly help to reduce the observed data spread.

The doses that were applied in the highlighted clinical studies where HRF were also observed, were approximately 5 times,[6] 10 times[7] and a 100 times[8] lower than the high dose in the present study. Although we do not have direct evidence, it seems plausible to assume that the diseased retina in those patients from the cited clinical studies might be more susceptible to additional inflammatory stimuli given the pre-existing retinal condition (in contrast to the healthy retina in primates).

Nevertheless, the nature of the HRF remains unclear. Previous studies have proposed potential explanations with regard to the nature of HRF in the outer retinal layers in different diseases, such as immune cell infiltration[8,23] or migrated RPE cells.[5,8,14] It is also known that microglia cells participate in inflammatory responses[10] and, hence, the presence of this cell type in different retina layers can be presumed in our analysis. Although we could not perfectly align the virtual cross sections from SD-OCT B-scans with sections from the fixed eye cup, we tried to confirm whether HRF could be grossly correlated with infiltrating immune cells, microglia activation, or migrated RPE cells in terms of appearance, frequency, and location in the sham- and rAAV8-treated eyes.

Although B- and T-cells were mostly detected in the rAAV8-treated eyes of the high dose group (3 out of 4), they were almost not present in the two other and more clinically relevant group doses (1 out of 4 in the low-dose group). Perivascular and subretinal infiltrates of these kind of immune cell has also been reported in previous studies[2,8,24] but their function in the tissue is still unclear. Interestingly, these infiltrates were only found in animals belonging to the groups where the number of HRF did not decrease over time, in line with an ongoing adaptive immune response to rAAV8.

It is known that once microglia cells become active, they are able to rapidly proliferate and migrate to the borders of the neural retina and RPE layer and secrete cytokines and chemokines.[25] In our study, we observe that microglia were active in areas close to the retinotomy site where HRF were found, but inactive in areas outside the bleb (and without HRF). Furthermore, microglia activation was more evident in the high dose group of rAAV8-treated eyes where the number of HRF also increased over time, than in sham-treated eyes. In line with this, microglia cells were recently shown to accumulate in the ONL in AMD.[26] We found it difficult to consistently detect HRF in layers outside the ONL (interclass correlation between masked observers <40%), which might be simply due to the fact that other layers show higher reflectivity compared to the relatively "dark" appearance of the ONL providing high contrast to HRF. In turn, this could mean that microglia cells might very well be located in the photoreceptor RPE layers but without being detected as discreet HRF on SD-OCT scans due to their reflectivity and also in other inner layers of the retina, as shown in our histology data (HRF in inner retinal layers were not evaluated).

The damage that is produced in the tissue upon subretinal injection can also induce morphological changes in the retina, such as thinning of the ONL due to the loss of the photoreceptors,[13] or the migration of RPE cells into the neural retina.[5,8] In our study, the thinning of the ONL that was observed appears to be due to the subretinal injection and not due to the rAAV8 as it was observed mainly in the sham-treated eyes. Regarding the migration of RPE cells, we could not find evidence of RPE cells within the neurosensory retina in histological sections that might explain HRF in the ONL on SD-OCT. An area of RPE layer was absent in the rAAV8-treated eye of only one animal of group 1 where the subretinal injection was performed. Indeed, the absence of the RPE monolayer, one of the building blocks of the blood retina barrier, might have contributed to the subretinal immune cell infiltration detected in this area.[27]

Taken together, an immune response to rAAV8 appears to be the most plausible explanation for the group of animals injected with the high dose and the HRF observed on SD-OCT could represent activated microglia migration into outer retinal layers. It is also noteworthy that the groups treated with more clinically relevant doses of rAAV8 (low and medium dose) did not show significant differences between sham- and rAAV8-treated eyes. Increasing or persistently high numbers of HRF on SD-OCT may indicate sustained retinal inflammation. Steroids or other immunomodulatory agents have been demonstrated as successful ways to manage gene therapy associated inflammation after subretinal injection of rAAV vectors. For that reason, the understanding of the kinetics of HRF could allow us to modulate the doses of steroids that are given to the patients in order to avoid constant retinal inflammation.

Acknowledgments

References

1. Bainbridge JWB, Mehat MS, Sundaram V, et al. Long-term effect of gene therapy on Leber's congenital amaurosis. *N Engl J Med*. 2015;372(20):1887–1897.

2. Boyd RF, Boye SL, Conlon TJ, et al. Reduced retinal transduction and enhanced transgene-directed immunogenicity with intravitreal delivery of rAAV following posterior vitrectomy in dogs. *Gene Ther*. 2016;23(6):548–556.

3. Fischer MD. On retinal gene therapy. *Ophthalmologica*. 2016;236(1):1–7.

4. Ye G, Budzynski E, Sonnentag P, et al. Safety and biodistribution evaluation in cynomolgus macaques of rAAV2tYF-PR1.7-hCNGB3, a recombinant AAV vector for treatment of achromatopsia. *Hum Gene Ther Clin Dev*. 2016;27(1):37–48.

5. Bucher K, Rodríguez-Bocanegra E, Dauletbekov D, Fischer MD. Immune responses to retinal gene therapy using adeno-associated viral vectors – Implications for treatment success and safety [published online ahead of print October 15, 2020]. *Prog Retin Eye Res*, https://doi.org/10.1016/j.preteyeres.2020.100915.

6. Cehajic-Kapetanovic J, Xue K, Martinez-Fernandez de la Camara C, et al. Initial results from a first-in-human gene therapy trial on X-linked retinitis pigmentosa caused by mutations in RPGR. *Nat Med*. 2020;26(3):354–359.

7. Dimopoulos IS, Hoang SC, Radziwon A, et al. Two-year results after AAV2-mediated gene therapy for choroideremia: the Alberta Experience. *Am J Ophthalmol*. 2018;193:130–142.

8. Reichel FF, Dauletbekov DL, Klein R, et al. AAV8 can induce innate and adaptive immune response in the primate eye. *Mol Ther*. 2017;25(12):2648–2660.

9. Liu YF, Huang S, Ng TK, et al. Longitudinal evaluation of immediate inflammatory responses after intravitreal AAV2 injection in rats by optical coherence tomography. *Exp Eye Res*. 2020;193:107955.

10. Coscas G, De Benedetto U, Coscas F, et al. Hyperreflective dots: a new spectral-domain optical coherence tomography entity for follow-up and prognosis in exudative age-related macular degeneration. *Ophthalmologica*. 2012;229(1):32–37.

11. Vujosevic S, Bini S, Midena G, Berton M, Pilotto E, Midena E. Hyperreflective intraretinal spots in diabetics without and with nonproliferative diabetic retinopathy: an in vivo study using spectral domain OCT. *J Diabetes Res*. 2013;2013: 491835.

12. Vujosevic S, Berton M, Bini S, Casciano M, Cavarzeran F, Midena E. Hyperreflective retinal spots and visual function after anti-vascular endothelial growth factor treatment in center-involving diabetic macular edema. *Retina*. 2016;36(7):1298–1308.

13. Xiong W, Wu DM, Xue Y, et al. AAV cis-regulatory sequences are correlated with ocular toxicity. *Proc Natl Acad Sci USA*. 2019;116(12):5785–5794.

14. Schuman SG, Koreishi AF, Farsiu S, ho Jung S, Izatt JA, Toth CA. Photoreceptor layer thinning over drusen in eyes with age-related macular degeneration imaged in vivo with spectral-domain optical coherence tomography. *Ophthalmology*. 2009;116(3):488–496.

15. Tannenbaum J, Bennett BT. Russell and Burch's 3Rs then and now: the need for clarity in definition and purpose. *J Am Assoc Lab Anim Sci*. 2015;54(2):120–132,

/pmc/articles/PMC4382615/?report=abstract. Accessed December 16, 2020.

16. Fischer MD, Hickey DG, Singh MS, MacLaren RE. Evaluation of an optimized injection system for retinal gene therapy in human patients. *Hum Gene Ther Methods*. 2016;27(4):150–158.

17. Vujosevic S, Bini S, Torresin T, et al. Hyperreflective retinal spots in normal and diabetic eyes: B-scan and en face spectral domain optical coherence tomography evaluation. *Retina*. 2017;37(6):1092–1103.

18. Kon Y, Iida T, Maruko I, Saito M. The optical coherence tomography-ophthalmoscope for examination of central serous chorioretinopathy with precipitates. *Retina*. 2008;28(6):864–869.

19. Turgut B, Yildirim H. The causes of hyperreflective dots in optical coherence tomography excluding diabetic macular edema and retinal venous occlusion. *Open Ophthalmol J*. 2015;9(1):36–40.

20. Berasategui B, Fonollosa A, Artaraz J, et al. Behavior of hyperreflective foci in non-infectious uveitic macular edema, a 12-month follow-up prospective study. In: *BMC Ophthalmology*. Vol. 18. London, England, UK: BioMed Central Ltd.; 2018.

21. Hanumunthadu D, Rasheed M, Goud A, Gupta A, Vupparaboina K, Chhablani J. Choroidal hyper-reflective foci and vascularity in retinal dystrophy. *Indian J Ophthalmol*. 2020;68(1):130–133.

22. Li Q, Miller R, Han PY, et al. Intraocular route of AAV2 vector administration defines humoral immune response and therapeutic potential. *Mol Vis*. 2008;14:1760–1769, /pmc/articles/PMC2559816/. Accessed March 26, 2021.

23. Bolz M, Schmidt-Erfurth U, Deak G, Mylonas G, Kriechbaum K, Scholda C. Optical coherence tomographic hyperreflective foci. A morphologic sign of lipid extravasation in diabetic macular edema. *Ophthalmology*. 2009;116(5):914–920.

24. Ramachandran PS, Lee V, Wei Z, et al. Evaluation of dose and safety of AAV7m8 and AAV8BP2 in the non-human primate retina. *Hum Gene Ther*. 2017;28(2):154–167.

25. Langmann T. Microglia activation in retinal degeneration. *J Leukoc Biol*. 2007;81(6):1345–1351.

26. Fletcher EL. Contribution of microglia and monocytes to the development and progression of age related macular degeneration. *Ophthalmic Physiol Opt*. 2020;40(2):128–139.

27. Crane IJ, Liversidge J. Mechanisms of leukocyte migration across the blood-retina barrier. *Semin Immunopathol*. 2008;30(2):165–177.